X-ray Crystallography and Solid-State NMR as Complementary Tools: Characterization of Novel Methylene Meldrum's Acid Precursors

Mohammad Zia-Ebrahimi,* Susan M. Reutzel,* Douglas E. Dorman, Larry A. Spangle, and Jack B. Deeter

*Lilly Research Laboratories, Eli Lilly and Company, Indianapolis, Indiana 46285*

Received December 30, 1993. Revised Manuscript Received April 11, 1994[●]

^{13}C CP/MAS NMR and X-ray crystallography are used to characterize the structures of novel methylene Meldrum's acid precursors. Correlations are made between specific structural elements found in the X-ray crystal structure of I and its solid-state NMR spectrum. The complementary use of solid-state NMR is demonstrated as the structures of related analogs, II–IV, for which X-ray structures are not available, are characterized using these correlations.

Introduction

Materials chemistry as a science has grown at the rate that methods have become available to characterize solids on a microscopic and a molecular level. While X-ray crystallography has traditionally been used to characterize molecular structure in the solid state, this technique has been limited in many cases by the difficulty associated with growing high quality single crystals. More recently, solid-state NMR has been demonstrated to be a reliable tool for studying intra- and intermolecular structure in the solid state.[1] Consequently, interest in the physical and chemical properties of solids has increased dramatically in recent years. Since single crystals are not required for solid-state NMR, this technique complements X-ray crystallography quite effectively.[2]

In our exploration of the use of solid-state NMR for characterizing solids, we investigated methylene Meldrum's acid precursors I–IV, which were prepared for the synthesis of geminal dicarboxy substituted amino acids.[3]

I   II   III   IV
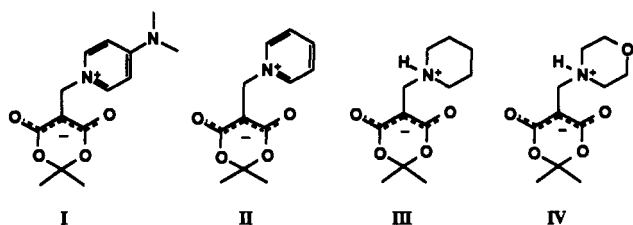
[●] Abstract published in *Advance ACS Abstracts,* May 15, 1994.

(1) (a) Etter, M. C.; Hoye, R. C. *Trans, ACA* 1986, *108*, 31. (b) Etter, M. C.; Urbanczyk-Lipkowska, Z.; Jahn, D. A.; Frye, J. S. *J. Am. Chem. Soc.* 1986, *108*, 5871. (c) Etter, M. C.; Vojta, G. M. *J. Mol. Graph.* 1989, *7*, 3.

(2) (a) Byrn, S. R.; Tobias, B.; Kessler, D.; Frye, J. S.; Sutton, P.; Saindon, P.; Kozlowski, J. *Trans ACA*, 1988, *24*, 41. (b) Glaser, R.; Maartman-Moe, K. *J. Chem. Soc.,* Perkin *Trans.* 1990, 2, 1205. (c) Stoltz, M.; Otiver, D. W.; Wessels, P. L.; Chalmers, A. A. *J. Pharm. Sci.* 1991, *80*, 357. (d) Ball, R. G.; Baum, M. W. *J. Org. Chem.,* 1992, *57*, 801.

(3) Methylene Meldrum's acid, shown below, is typically generated *in situ* and is rather unstable:
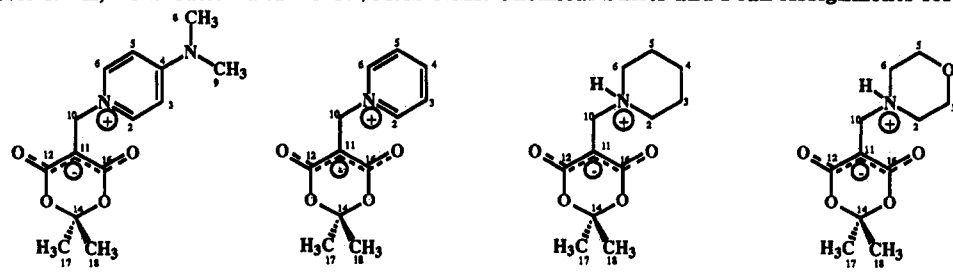

Compounds I–IV represent the first examples of stable methylene Meldrum's acid precursors. The synthetic utility and features of these compounds will be reported in an upcoming paper.

The structure of I initially characterized by solution NMR, was confirmed by X-ray crystallography. Derivatives II–IV, however, failed to yield high-quality crystals, thus prohibiting their crystal structures from being determined. Therefore, specific features in the solid-state NMR spectrum of I were correlated to structural information obtained from the X-ray data and these correlations were subsequently applied to identify similar solid-state structural features in II–IV. Herein we report the X-ray structure of I and the spectroscopic characterization of I–IV using solution- and solid-state NMR.

Experimental Section

Synthesis. For the synthesis of I, III, and IV, Meldrum's acid was reacted with 1 equiv of the appropriate base and 1 equiv of 37% aqueous formaldehyde in absolute ethanol at 25 °C. In the case of I, the reaction mixture was concentrated *in vacuo* after 15 h. The remaining yellow oil was triturated with 1:1 diethyl ether/hexane. The solvent was then evaporated under a gentle stream of nitrogen to produce I as a white crystalline solid. For the synthesis of II, Meldrum's acid was dissolved in 10-fold excess of pyridine, followed by the addition of 1 equiv of aqueous formaldehyde. The mixture was stirred at 25 °C for 1 h, concentrated *in vacuo* to give a yellow crystalline solid which was stirred with hexanes for 15 min, and filtered. In the case of III and IV, the respective products were formed as white precipitates after about 2 h, filtered, and used without any further purification. It should be noted that all of these derivatives in the presence of aqueous acids and water will decompose to methylene Meldrum's acid and the respective base; therefore, appropriate precautions should be taken.

Solution- and Solid-State NMR. ^{1}H and ^{13}C NMR spectra of I–IV were obtained in $CDCl_3$ or $CDCl_3$/DMSO-d_6 on a Bruker AC250 and are reported in ppm relative to TMS. ^{13}C CP/MAS NMR spectra were obtained using a Bruker AC250 spectrometer operating at a carbon frequency of 62.897 MHz and equipped with a Bruker solid-state accessory and probe. Typical measurement conditions were as follows: 90° proton rf pulse 8 μs, contact time 1 ms, pulse repetition time 5 s, MAS frequency 4.8–5.2 kHz, spectral width 15 kHz, and acquisition time 34 ms. The ^{13}C chemical shifts were referenced to the CH_2 of adamantane (δ = 38.3 ppm) by sample replacement. Dipolar dephased spectra were measured with a 50-μs delay without decoupling prior to acquisition. Spectral assignments were made by comparing chemical shifts observed in solution spectra with those in the ^{13}C CP/MAS and dipolar dephased spectra and are given in Table 1.

Table 1. ^{1}H, ^{13}C Solution and ^{13}C CP/MAS NMR Chemical Shifts and Peak Assignments for I–IV

assignment	^{1}H	$^{13}C_{soln}$	$^{13}C_{solid}$	^{1}H	$^{13}C_{soln}$	$^{13}C_{solid}$	^{1}H	$^{13}C_{soln}$	$^{13}C_{solid}$	^{1}H	$^{13}C_{soln}$	$^{13}C_{solid}$
17, 18	1.64	25.75	27.9, 29.3	1.67	25.78	23.2, 27.8	1.64	26.01	25.3, 29.2	1.63	25.74	24.7, 29.4
8, 9	3.20	39.53	35.6, 36.7									
			39.1, 39.9									
10	5.01	55.68	53.8	5.53	63.01	58.1	3.84	54.78	52.1	3.92	55.09	54.6
11		71.52	73.9		73.14	73.8		67.01	68.9		66.14	66.9
14		101.50	102.0		102.12	102.0		101.71	100.6		101.61	100.5
3,5	6.68	106.79	102.7, 111.3	7.83	126.58	127.2, 132.2	1.85, 2.02	22.43	22.9	3.99	63.18	64.3, 65.9
2,6	8.33	141.86	143.7	9.06	144.64	145.0	2.72, 3.50	52.24	54.9, 56.8	2.99, 3.38	50.78	51.1, 51.9
4		155.84	154.7, 155.9	8.25	142.21	143.5	1.43, 1.85	22.29	22.9			
12, 16		166.96	167.3, 167.9		166.64	166.4		167.59	166.4, 167.8		167.18	166.5, 168.7
NH							9.36			9.90		

Table 2. Crystallographic Data for the X-ray Structure of I

formula	$C_{14}H_{18}N_2O_4$		0.779
formula weight	278.31		22(1)
space group	$P2_12_12_1$	no. of unique data	1114
a (Å)	7.1270(10)	no. of data used	1039
b (Å)	10.044(3)	R^a	0.073
c (Å)	19.322(7)	$R_w{}^b$	0.111
V (Å^3)	1383.2(7)	$2\theta_{max}$ (deg)	116.0
Z	4	range of hkl	$-7 \leq h \leq 0$
d_{calc} (g/cm^3)	1.336		$-10 \leq k \leq 0$
	μ(Cu Kα) (mm^{-1})		$0 \leq l \leq 20$
	T °C	(shift/error)$_{max}$	0.04
		largest peak (e Å^{-3})	0.26

$^a R = \Sigma(F_{obs} - F_{calc}/\Sigma(F_{obs}).^b R_w = \Sigma[(F_{obs} - F_{calc})\sqrt{weight}/\Sigma[(F_{obx})\sqrt{weight}]$.

Crystal Structure Determination of I. Colorless prisms of I were grown from acetonitrile by slow evaporation at 25 °C. Crystal data were collected on a Siemens R3m/V diffractometer with graphite monochromated Cu Kα radiation (λ = 1.541 78 Å) using the 2θ–θ scan technique. The structure was solved by direct methods using Siemens SHELXTL PLUS.[4] All non-hydrogen atoms were refined anisotropically. All hydrogens were included in structure factor calculations and placed in idealized positions (d_{C-H} = 0.95 Å) with assigned isotropic thermal parameters (B = 1.2B of bonded atoms). The experimental details of the X-ray analysis are given in Table 2.

Results and Discussion

Spectroscopic and Crystallographic Analysis of I. Solid-state NMR has proven to be a powerful tool for studying molecular structure, yet X-ray crystallography remains the unanimous choice for characterizing crystalline solids. The primary advantage of using crystallography over solid-state NMR is that the structure parameters, such as intra- and intermolecular bond lengths and angles, can be precisely determined, thus giving a "direct" picture of the molecular structure and organization.[5] The main disadvantage of crystal structure analysis, however, is the requirement of high-quality single crystals as substrates. Thus, solid-state NMR complements X-ray crystallography for the structural characterization of polycrystalline and amorphous materials and mixtures of solid phases.[2c]

Solid-state NMR spectra of microcrystalline powders often differ from the corresponding spectra in solution and usually appear to be more complex. The differences reflect not only the dissimilar electronic environments in solution and solid state but also the different motional freedom of molecules in the respective phases. In this study, we systematically dissect the solid-state NMR spectra of I–IV and find that a wealth of information pertaining to molecular configuration, symmetry, molecules per asymmetric unit, conformations, electronic structure, and intermolecular interactions can be obtained.

The structure of I was initially assigned in solution by ^{1}H and ^{13}C NMR. Since only nine resonances are seen in its ^{13}C NMR spectrum and five in its ^{1}H NMR spectrum, a symmetrical structure having an internal mirror plane is proposed. Substitution at C11 is confirmed by the large chemical shift change at this site (71.52 ppm) relative to its position in Meldrum's acid (35.20 ppm). The chemical shifts of this sp^2 hybridized center and the carbonyl carbons further reveal that the malonate moiety is fully delocalized and negatively charged.

The molecular structure of I initially assigned by solution NMR was confirmed by X-ray crystallography. Compound I, which possesses a mirror plane under its ideal point group symmetry, is seen to lose that symmetry when crystallized in the $P2_12_12_1$ space group (Figure 1). The sp^2 hybridization of C11, as indicated by the 360.0(4)° sum of the bond angles about this atom, causes the Meldrum's ring in I to adopt a half-boat conformation. In this conformation, the isopropylidene methyl groups are nonequivalent: one is pseudoaxial and the other is

(4) Sheldrick, G. M. Siemens Crystallographic Research Systems, New Jersey, 1990; Release 4.1. For Siemens R3m/V Crystallographic Systems.

(5) (a) Etter, M. C.; Hoye, R. C.; Vojta, G. M. *Cryst. Rev.* **1988,** *1*, 281 and references therein. (b) Etter, M. C.; Reutzel, S. M.; Vojta, G. M. *J. Mol. Struct.* **1990,** *237*, 165. (c) Saito, H. *Magn. Reson. Chem.* **1986,** *24*, 835. (d) Hays, G. R. *J. Chem. Soc., Perkin Trans. 2* **1983,** 1049. (e) Hays, G. R.; Huis, R.; Coleman, B.; Clague, D.; Verhoweven, J. W.; Rob, F. *J. Am. Chem. Soc.* **1981,** *103*, 5140. (f) Clayden, N. J.; Dobson, C. M.; Lian, L.-Y.; Twyman, J. M. *J. Chem. Soc., Perkin Trans 2* **1986,** 1933. (g) Liang, T.-M.; Laali, K. K. *Chem. Ber.* **1991,** *124*, 2637. (h) Likar, M. D.; Taylor, R. J.; Fagerness, P. E.; Hiyama, Y.; Robins, R. H. *Pharm. Res.* **1993,** *10*, 75.

(6) Deleted in proof.

824 *Chem. Mater., Vol. 6, No. 6, 1994*
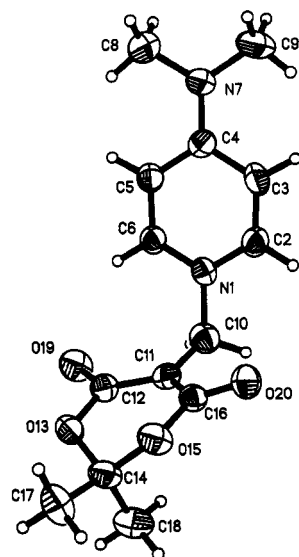
Zia-Ebrahimi et al.

Figure 1. Molecular geometry of **I**, showing the loss of mirror symmetry in the crystal. Thermal ellipsoids are depicted at 50% probability.

pseudoequatorial. The C6–N1–C10–C11 torsion angle of 68.1° forces the mirror plane bisecting C17, C18, C14, C11, C10, N1, C4, and N7 to be destroyed. Thus the dimethylamino methyl (C8, C9), the pyridinium ring (C2, C6 and C3, C5), and the malonate carbonyl carbons (C12 and C16) are also rendered inequivalent in the solid state.

The formation of a betaine structure not only causes dramatic changes in the molecular conformation of the Meldrum's acid ring in **I** but also greatly affects the carbonyl and internal C–C bond lengths. The C–O bond lengths of 1.229(6) Å (C16–O20) and 1.223(6) Å (C12–O19) are slightly longer than those of isolated carbonyl groups[7] and the C–C bond lengths of 1.405(7) Å (C11–C12) and 1.392(7) Å (C11–C16) are intermediate between those of carbon–carbon single and double bonds. These lengths reflect the deprotonation and enolization of the malonate moiety. Their equivalency further indicates that the malonate π-system is completely delocalized.[8]

Since there are four molecules in the unit cell,[9] only one molecule is present in the asymmetric unit of this structure. The cationic and anionic sites in each molecule of **I** are partitioned in the crystal. Positively charged pyridinium rings are π-stacked along the *a* axis in the crystal (Figure 2). The interplanar spacing between pyridinium rings of
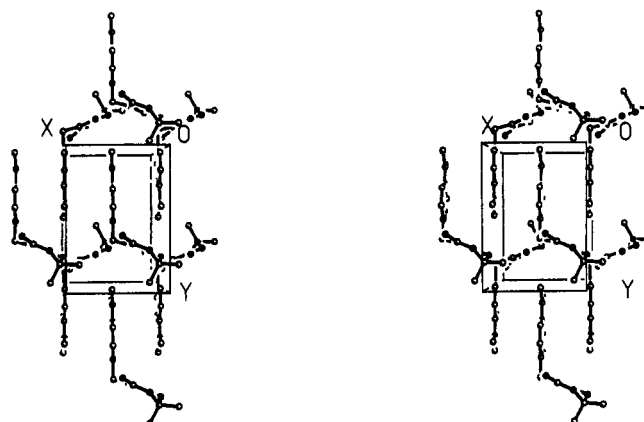
(7) The C=O bond lengths in Meldrum's acid are 1.187(4) and 1.199-(4) Å. Pfluger, C. E.; Boyle, P. D. *J. Chem. Soc., Perkin Trans 2* **1985**, 1547.

(8) The structure of a completely delocalized lithium 1,3-cyclohexanedione enolate has recently been reported in which the C–C bond lengths (1.396(4) and 1.393(3) Å) and the C–O bond lengths (1.268(3) and 1.263-(3) Å) were identical despite the very different solid-state environments of the carbonyl groups. The slightly longer C–O bond lengths may be attributed to intermolecular interactions with the solvent. Etter, M. C.; Ranawake, G.; *J. Am. Chem. Soc.* **1992**, *114*, 4430.

(9) In the space group $P2_12_12_1$ there are four symmetry-related asymmetric units per unit cell. In the structure of **I** the number of molecules per unit cell, which is given by Z, is 4. Therefore, in this structure there is one molecule per asymmetric unit.

Figure 2. Stereoview of the unit cell of **I** viewed along [001], showing the π-stacking of DMAP rings in the crystal and the partitioning of cationic and anionic layers.
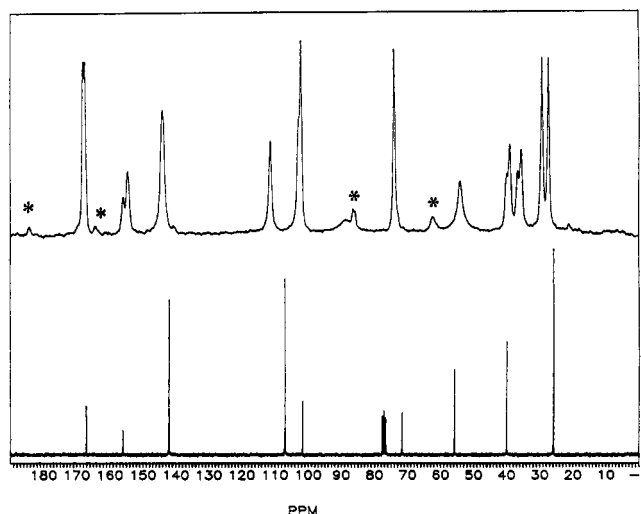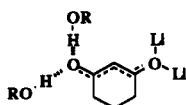

Figure 3. ^{13}C NMR spectra of **I** in the solid state (top) and in CDCl₃ (bottom). Spinning side bands are denoted by asterisks.

neighboring screw-related molecules is 3.564 Å.[10] The positive charges on the pyridinium rings are offset by the negatively charged malonates aligned in adjacent layers, yet the crystal structure shows no evidence of specific ionic interactions.

Many features in the crystal structure of **I** could be identified in its ^{13}C CP/MAS NMR spectrum, which shows relatively sharp lines as expected for a highly crystalline material (Figure 3). For example, solid-state NMR clearly reveals the molecular asymmetry of **I** in the crystal. In solution, rapid conformational interconversion and ring flipping motions cause the carbons related by the internal mirror plane to become degenerate. Since molecular motion and ring interconversion are much slower or even impossible in the crystal relative to in solution, the nominally equivalent carbons in solution are rendered inequivalent in the solid. Therefore, the splitting of peaks due to methyl carbons, C8, C9, and C17, C18, in the solid-state NMR spectrum of **I** may be attributed to their crystallographic inequivalence. Similar splittings are also seen for the pyridinium C3 and C5 carbons. The C2 and C6 peaks are not resolved, however.

(10) This distance was calculated by dividing the distance between the mean planes of the translationally related rings by 2. The distance was measured in Quanta, version 3.3, Molecular Simulations, Inc.

Molecular asymmetry accounts for the doubling of many of the carbon signals in the solid-state NMR spectrum, yet several of the peaks experience splitting which cannot be explained solely on these grounds. Another cause of splitting is the residual dipolar coupling between ^{13}C and quadrupolar ^{14}N nuclei,[11] which affects the peaks of carbons in close proximity to nitrogens. Quadrupolar [14]N–[13]C is characterized by broadening (C2, C6, C10) and/or splitting of the ^{13}C peaks into asymmetric doublets (C4, C8, C9). These often diagnostic peak shapes are useful for making peak assignments for carbons near nitrogen atoms in the solid state. Because only one peak (or one asymmetric doublet) is seen for each different carbon in the unsymmetrical molecules of I, ^{13}C CP/MAS NMR supports the X-ray crystal structure finding of only one molecule per asymmetric unit.

The completely delocalized malonate moiety in I, as revealed by the similar C–O and internal C–C bond lengths found by X-ray diffraction, is also supported in its solid-state NMR spectrum. The carbonyl carbons appear as two peaks in the ^{13}C CP/MAS NMR spectrum as would be expected in a localized structure; however, their nearly identical chemical shifts suggest a delocalized structure.[12] The small splitting (0.6 ppm) of the C12 and C16 peaks is attributed to the crystallographic inequivalence of these carbons. Consequently, not only does solid-state NMR show that the enolate moiety is considerably delocalized, but it also reveals the small differences between the environments of the two carbonyl groups in the crystal.

Spectroscopic Analysis of II–IV. The solid-state NMR spectra of II–IV, for which crystal structures have yet to be determined, were interpreted in terms of the specific structural elements found in the X-ray structure of I and established in its solid-state NMR spectrum. The molecular structure of the unsaturated analog II, for example, was readily identified as a betaine similar to I both in solution and in the solid state based on the comparable chemical shifts of these derivatives in both phases. Because the saturated analogs, III and IV, have an acidic hydrogen, the molecular structures of these derivatives cannot be assumed to be the analogous zwitterion, A. Alternative structures are also possible for

A   B   C
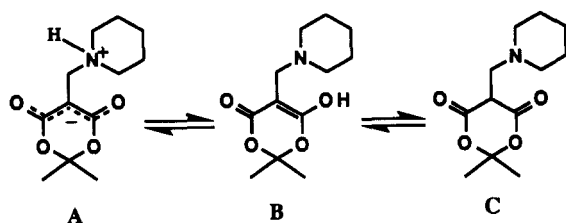
these derivatives. Proton transfer to effectively neutralize the charged centers of the zwitterionic form of III (and IV) could lead to the enolamine, B. Molecule B can further tautomerize to form a diketo structure, C.

Which, if any, of the possible molecular structures of III (and IV) predominates in solution was readily identi-

fied using NMR. Structure C was immediately ruled out because acidic protons near 9.5 ppm were seen in the ^{1}H NMR spectra of each of these analogs. A hydrogen at C11 would be expected to appear farther upfield at about 3–4 ppm. Using selective irradiation experiments, B was also eliminated as a possible structure since coupling was detected between the acidic hydrogen at 9.5 ppm and the C10 protons at 2.7 ppm. This three-bond coupling between the 9.5 ppm proton and the C10 hydrogens is feasible only for the zwitterionic structure, A. Additional evidence for structure A was provided by ^{13}C NMR, for which C11, C12, and C16 carbon chemical shifts comparable to those found in I and II are seen. The combined use of ^{1}H and ^{13}C NMR therefore revealed that III-A (and IV-A) predominates in solution.

The molecular structures of III and IV in the solid state were subsequently identified using dipolar dephased NMR,[13] a solid-state NMR spectral editing technique which provides subspectra of only quaternary and rapidly spinning methyl resonances, and by comparing the solution- and solid-state chemical shifts of these analogs. Dipolar dephasing immediately revealed that C11 is a quaternary center in III and IV, since the peaks at ~70 ppm are retained in their subspectra. This proves that III-C and IV-C are not present in the solid state. The similar chemical shifts of C11, C12, and C16 observed in the solid-state spectra of III and IV relative to in solution further reveals that their malonate π systems are negatively charged and delocalized, thus ruling out structure B in the solid state. All solid-state chemical shifts and hybridization assignments are indeed consistent with III-A (and IV-A).

Molecular asymmetry and the absence of multiple molecules per asymmetric unit seen in the crystal structure of I and established in its solid-state NMR spectrum were also ascertained from the solid-state NMR spectra of analogs II–IV. Thus, the ^{13}C peaks of nominally equivalent carbons in solution (e.g., C3, C5 or C12, C16), which were split in the solid-state NMR spectrum of I, appear as distinct resonances in II–IV. Similarly, different carbons in the unsymmetrical molecules of II–IV are seen as single peaks, or asymmetric doublets, indicating that there is only one molecule per asymmetric unit in each unit cell.

The absence of molecular mirror symmetry, which imparts crystallographic inequivalence on the malonate carbonyl carbons, only partially explains the chemical shift differences between these nuclei in III and IV. The significantly different (~2 ppm) chemical shifts may also be attributed to either crystal packing forces or hydrogen bonding, presumably between the NH of the piperidine (or morpholine) and one of the carbonyl oxygens, thus moving the corresponding carbon peak downfield. Interestingly, even if one of the carbonyl groups is hydrogen-bonded, the malonate moiety appears to be extensively delocalized given that the chemical shifts are in the range of those observed in I. Whether the hydrogen-bonding interaction(s) is inter- or intramolecular, or both, is not clear from the spectroscopic data alone. An X-ray structure is required to establish the exact hydrogen-bonding pattern.

(11) (a) Hexem, J. G.; Frey, M. H.; Opella, S. J. *J. Chem. Phys.* 1982, 77(7), 3847. (b) Hexem, J. G.; Frey, M. H.; Opella, S. J. *J. Am. Chem. Soc.* 1981, 103, 224. (c) Olivieri, A. C.; Frydman, L.; Diaz, L. E. *J. Magn. Reson.* 1987, 75, 50.

(12) The carbonyl carbons in lithium enolates of 1,3-cyclohexanedione are also seen as one peak in the solid-state NMR spectrum, confirming that they are electronically equivalent. See ref 9.

(13) Opella, S. J.; Frey, M. H. *J. Am. Chem. Soc.* 1979, 101, 5854.

Conclusions

We have shown how effective and powerful the combined use of solid-state NMR and X-ray crystallography can be for characterizing molecular solids. Several elements of crystal structure, including configuration, conformation and symmetry were readily deduced for materials without X-ray structures. While solid-state NMR will not replace X-ray crystallography as a structure characterization tool, it can provide otherwise unattainable information for many types of materials, and therefore this technique should be a part of any materials characterization program.

Supplementary Material Available: Tables of positional parameters and anisotropic thermal parameters and intramolecular bond lengths and angles and unit cell drawings (6 pages); tables of observed and calculated structure factors (4 pages). Ordering information is given on any current masthead page.